



## Area-Selective ALD of Titanium Dioxide Using Lithographically Defined Poly(methyl methacrylate) Films

Ashwini Sinha, Dennis W. Hess,\* and Clifford L. Henderson\*\*<sup>z</sup>

School of Chemical and Biomolecular Engineering, Georgia Institute of Technology,  
Atlanta, Georgia 30332-0100, USA

An approach to area-selective atomic layer deposition techniques based on the use of a lithographically definable polymeric masking layer has been reported. Successful direct patterned deposition of TiO<sub>2</sub> is demonstrated using a poly(methyl methacrylate) masking layer that has been patterned using deep-UV lithography. A number of factors which must be considered in designing patternable polymeric masking materials and processes have been determined and are briefly discussed, including reactivity of the polymer with the atomic layer deposited (ALD) precursor species, diffusion of ALD precursors through the polymer mask, and remnant precursor content in the masking film during ALD cycling.

© 2006 The Electrochemical Society. [DOI: 10.1149/1.2184068] All rights reserved.

Manuscript submitted May 26, 2005; revised manuscript received December 12, 2005. Available electronically March 27, 2006.

Atomic layer deposition (ALD) is gaining significant attention as an alternative technique for depositing high-quality, ultrathin films.<sup>1,2</sup> This method is particularly useful for producing extremely thin, high-quality, conformal films with thicknesses in the 3–10 nm range where other deposition techniques such as chemical vapor deposition (CVD) have significant limitations. During ALD, film growth depends critically on the chemistry of the surface upon which deposition occurs. Thus, it should be possible to chemically tailor a surface to achieve area-selective deposition. Selective ALD requires that designated areas of the surface be masked or “protected” to prevent the ALD reaction from occurring in those selected areas, thus ensuring that the ALD film nucleates and grows only on the desired unprotected regions. One obvious advantage of such an additive, area-selective deposition process is the ability to perform direct patterned growth, thereby eliminating the need for etching and the associated subsequent cleaning steps. Elimination of these steps can greatly simplify the overall deposition and patterning process, reduce unintended damage to substrates and devices which result from the use of energetic plasma etch processes, and aid in the integration and patterning of new materials which are difficult to etch.

The critical challenge in achieving area-selective ALD is devising materials and methods for modifying selected regions of a substrate surface to prevent ALD reactions from occurring, thus preventing film growth. One way to modify a surface is to chemically bond a molecule directly to the surface. Such an approach blocks reactive sites that are present and thereby prevents reactions between precursor molecules and the surface. Alkyl silanes, which contain long hydrocarbon chains terminated with a reactive silane end group, are a well-known surface-modifying agent. In the case of alkyl silanes, the hydrocarbon chains are relatively unreactive and thus provide a good protective or passivating coating for the surface. For example, octadecyltrichlorosilane (OTS) forms a densely packed, self-assembled monolayer (SAM) and has been widely investigated as a surface-modifying agent to block nucleation and growth of a variety of inorganic films such as HfO<sub>2</sub>, ZnO, TiO<sub>2</sub>, ZrO<sub>2</sub>.<sup>3-5</sup> Previous studies<sup>3,4</sup> have demonstrated direct patterned deposition of ZnO and TiO<sub>2</sub> on patterned SAM surfaces. However, the reaction selectivity, i.e., effectively the analog of resist contrast, for area-selective ALD between the SAM-modified and unmodified regions during ALD film growth was not adequately addressed in these studies. Recent studies<sup>5</sup> have reported that in the case of silicon surfaces, it is necessary to expose the silicon surface to the silane solution for more than 48 h in order to achieve a pinhole-free SAM layer that effectively blocks all reactive nucleation sites on the surface.

We have also investigated the use of OTS and other SAMs as surface-modifying agents for the area-selective ALD of titania onto silicon surfaces. In these studies, titania was deposited using alternating cycles of water and titanium tetrachloride vapors. During the first 50 cycles of titania deposition, nucleation of TiO<sub>2</sub> on the SAM surface was undetectable as measured using X-ray photoelectron spectroscopy (XPS). However, further increases in the number of deposition cycles resulted in detection of TiO<sub>2</sub> (~1.0–1.5 atom % after 100 cycles and 3–4 atom % after 150 cycles) on the SAM surface. These results suggest that the reactive titanium precursor eventually finds an unprotected reactive silanol site on the silicon surface and reacts to initiate the ALD reaction sequence in that area. Previous studies<sup>6-8</sup> which have investigated the mechanism of SAM formation have also reported the extreme difficulty and challenge associated with obtaining a “defect-free” monolayer. This difficulty with defectivity and undesired nucleation, coupled with the facts that SAM deposition is time-consuming and the high-resolution patterning of SAMs is not a well-established practice, pose serious limitations on the successful use of SAMs as masking layers for area-selective ALD.

Unlike SAMs, polymers can be quickly and easily spin coated to obtain defect-free thin films. This fact is exploited extensively in almost all modern microlithographic processes. Furthermore, a significant amount of research has been invested in developing a variety of different polymeric materials and processes for the high-resolution patterning of polymer films. Materials and processes exist for lithographically patterning a range of polymers including materials based on epoxies, novolac, poly(hydroxystyrene), poly(norbornene), polyacrylates, polyimides, and polycarbonates. Thus, if a polymer or class of polymers is identified that can prevent the nucleation and growth of a material on its surface during ALD and which can be patterned lithographically, such a “photoresist-like” process may offer a better alternative as a masking scheme for area-selective ALD as compared to SAM-based approaches. After the ALD is completed, the goal would be that the polymer masking layer is removed in the same way that resist films are stripped, thus obtaining the direct patterned structure of the desired ALD film. In fact, some related work has shown that polymeric masks (PMMA and AZ 5214 photoresist) can be used to achieve selective CVD of Cu lines onto a tungsten-coated Si substrate using 1,5-cyclooctadiene-Cu(I) hexafluoroacetylacetonate as a single precursor.<sup>9,10</sup>

Deposition of metal oxide films by ALD often uses water as an oxygen source and may involve highly reactive halides as metal precursors. Thus, identifying a polymer system which can successfully serve as a masking layer for area-selective deposition of metal oxides involves a number of challenges. A variety of issues such as the reactivity of the polymer with precursors, uptake of water and metal precursor by the polymer film, the presence of remnant precursor in the polymer masking film after the purge cycle, and the diffusion of ALD precursors through the polymer masking film can all affect the selective ALD process. Initial discussion and investi-

\* Electrochemical Society Fellow.

\*\* Electrochemical Society Active Member.

<sup>z</sup> E-mail: [cliff.henderson@chbe.gatech.edu](mailto:cliff.henderson@chbe.gatech.edu)

gation of the necessary criteria along with parametric data for the identification of effective masking materials for selective ALD can be found in a previous publication.<sup>11</sup> In this paper we report the successful use of a conventional photoresist poly(methyl methacrylate) or PMMA to obtain the direct patterned deposition of TiO<sub>2</sub> films using TiCl<sub>4</sub> and water as ALD precursors. Furthermore, we offer additional details concerning the effect of the various phenomena mentioned above on the prospects for a polymer masking-based, area-selective ALD process.

### Experimental

The ALD system consists of a six-way 2.75-in. conflat cross which serves as the reaction chamber. Samples are placed onto an aluminum plate which is heated using 1-in. CSH series cartridge heaters and the temperature is read with a K-type thermocouple. Ultrahigh-purity nitrogen is supplied through a rotameter and mixes with precursors before entering the reaction chamber. Nitrogen serves as both the carrier gas and purge gas for this ALD system. The chamber is evacuated with an Alcatel 2021SD rotary vane pump; chamber pressure is controlled by simultaneously varying the conductance of the pump via a throttle valve and the flow rate of nitrogen. Maximum conductance is used in order to achieve the maximum flow rate of nitrogen purge through the system. ALD is performed at a total pressure of 1 Torr with a total N<sub>2</sub> flow rate of 78 sccm. Pressure inside the chamber is monitored using a thermocouple-based vacuum pressure gauge connected to one port of the six-way cross. Precursors are introduced into the chamber in an alternating manner by using computer-controlled solenoid valves. A metering valve is also attached immediately upstream of each solenoid valve in order to control the total flow rate of each precursor. A liquid nitrogen trap placed between the chamber and vacuum pump prevents unreacted precursors and products from entering the pump.

Blanket film depositions were initially conducted in order to investigate system behavior and determine the operating conditions required to perform ALD using titanium tetrachloride and water as precursors for the deposition of TiO<sub>2</sub>. Titanium tetrachloride (99.9%) was purchased from Sigma-Aldrich and used as received for the titanium precursor source while deionized (DI) water was used as the oxygen precursor source. Both precursors were maintained at room temperature where the vapor pressures of TiCl<sub>4</sub> and H<sub>2</sub>O are 13 and 23 Torr, respectively. All depositions were conducted at a substrate temperature of 160°C and 1 Torr chamber pressure. Clean, p-type silicon (100) wafers were used as substrates. Wafers were thoroughly rinsed with acetone, methanol, isopropanol, and DI water to remove surface organics and then immersed in 2 M HNO<sub>3</sub> for 2 h to increase the surface hydroxyl concentration before ALD.<sup>12</sup> After removal from the HNO<sub>3</sub> solution, the wafers were rinsed again with DI water and dried under nitrogen before being loaded into the ALD chamber. The chamber was evacuated to base pressure of 40 mTorr and the deposition process was started after a further wait of 2 h. The ALD deposition cycle used consisted of (i) TiCl<sub>4</sub> pulse, (ii) N<sub>2</sub> purge, (iii) H<sub>2</sub>O pulse, and (iv) N<sub>2</sub> purge. PMMA films were spin coated onto Si wafers from a 1–5 wt % PMMA (Scientific polymer products, Mw = 54,000) polymer solution in toluene. The samples were soft-baked at 120°C for 5 min on a hot plate and then vacuum annealed at 100°C for 2 h to ensure removal of residual casting solvent.

**Film thickness measurements.**— Film thicknesses were measured using both spectroscopic ellipsometry and X-ray reflectivity. Spectroscopic ellipsometry measurements were performed with an M-2000 ellipsometer (J.A. Woollam Co., Inc.). Ellipsometry data were collected over a wavelength range from 400 to 1000 nm at angles of 65, 70, and 75° (with respect to normal to the substrate plane). Data were analyzed and fit to determine film thickness and refractive index using the WVASE-32 software package (J.A. Woollam Co.) by employing a Cauchy model for the films and using a standard silicon substrate library data file. X-ray reflectivity mea-

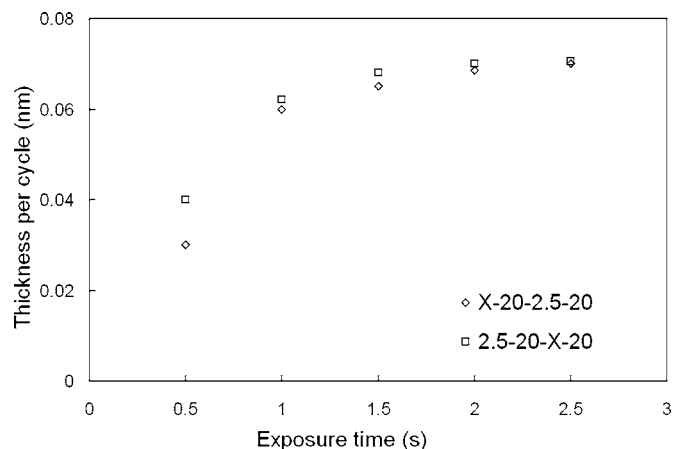


**Figure 1.** Thickness grown per ALD cycle vs exposure time for one of the precursors. The legend format refers to the time duration of each step in the ALD cycle. For example, “X-20-2.5-20” refers to an ALD sequence of (i) X seconds exposure of TiCl<sub>4</sub>, (ii) 20 s N<sub>2</sub> purge, (iii) 2.5 s exposure to water, and (iv) 20 s N<sub>2</sub> purge. The two different data sets are for varying the (□) water exposure time and the (◇) TiCl<sub>4</sub> exposure time.

surements were performed using an X’pertPRO X-ray diffraction (XRD) system (PANalytical, Inc.). For X-ray reflectivity experiments, copper radiation with wavelength of 1.54 Å was used with the X-ray source generator tension and current set at 45 kV and 40 mA, respectively. Samples were scanned at low incident angles from 0 to 3.0° with a step size of 0.005° and a time per step of 0.1 s. Data were analyzed using the X’pert reflectivity software which calculates the film thickness from the relative distance in angular position of the fringes in the reflectivity scans. Thicknesses measured using both techniques generally agreed to within ±0.2 nm.

**X-ray photoelectron spectroscopy (XPS).**— Chemical analysis of the films and surfaces was performed using XPS. XPS spectra were collected using a Physical Electronics (PHI) model 1600 XPS system equipped with a monochromator. The system used an Al Kα source ( $h\nu = 1486.8$  eV) operating at 350-W beam power. Ejected photoelectrons were detected by a hemispherical analyzer that provided both high sensitivity and resolution. The operating pressure in the sampling chamber was below  $5 \times 10^{-9}$  Torr. Samples were aligned in the beam by maximizing photoelectron counts corresponding to the primary C 1s peak in C–C bonds located at a binding energy of 284.8 eV. A neutralizer beam was used during XPS measurements to compensate for peak shifting which occurs due to charging of samples during X-ray exposure. All high-resolution spectra were collected using a pass energy of 46.95 eV. The step size and time per step were chosen to be 0.025 eV and 100 ms, respectively. Atomic concentrations of different elements were calculated based on the photoelectron intensities of each element and the elemental sensitivity factors provided by the tool manufacturer. Samples were scanned at different locations and the peak intensity and composition at different locations compared to assure uniformity of film composition over the sample surface. XPS spectra showed that the deposited films are generally free of contaminants to the level of detectability (~0.1 atom %). Titanium concentrations on the surface are of particular importance in this work; thus, the titanium signals were analyzed using the Ti 2p<sub>3/2</sub> peak at 458.8 eV, which is characteristic of titanium in TiO<sub>2</sub>.<sup>13</sup>

### Results

**Determination and verification of ALD process conditions.**— Figure 1 shows the growth rate of TiO<sub>2</sub> films as a function of varying exposure time for one of the precursors while maintaining a constant exposure time for the other precursor. The data suggest self-saturated reaction and growth of TiO<sub>2</sub> films at precursor expo-

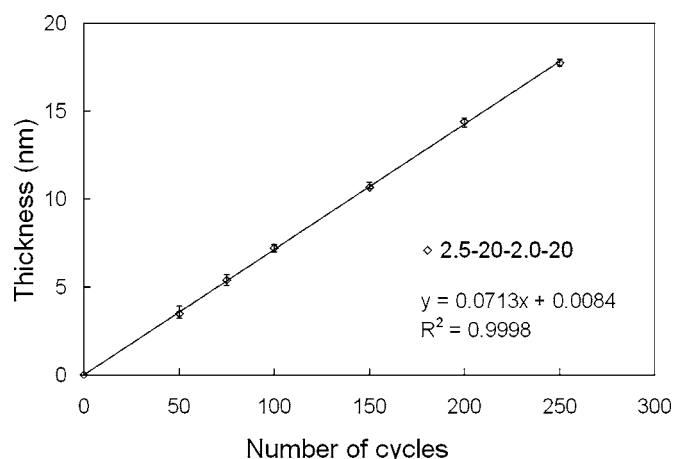


**Figure 2.** Thickness of the  $\text{TiO}_2$  film as a function of number of ALD cycles. The linear growth with number of cycles is indicative of an ALD process.

sure times for  $\text{TiCl}_4$  and water of at least 2.5 and 2.0 s, respectively, at  $160^\circ\text{C}$ . Under these conditions, the growth rate of  $\text{TiO}_2$  saturates at  $\sim 0.07$  nm per cycle, consistent with results reported previously.<sup>14,15</sup> Exposure times for  $\text{TiCl}_4$  and water vapor were thus fixed at 2.5 and 2.0 s, respectively, and  $\text{TiO}_2$  growth was performed at various numbers of cycles to verify the expected linear dependence of material growth with number of cycles for a true ALD process. Figure 2 demonstrates that the  $\text{TiO}_2$  film thickness is a linear function of the number of ALD cycles performed. Thus, self-saturated growth and a linear relationship with the number of growth cycles indicate that the above operating conditions provide deposition of  $\text{TiO}_2$  in an ALD mode.

**ALD growth studies on PMMA films.**— Initial experiments were conducted to test the suitability of PMMA films as a masking layer for the selective deposition of  $\text{TiO}_2$  using  $\text{TiCl}_4$  and water as precursors. Unlike SAM surfaces, polymer films can physically absorb reasonably large quantities of water. Absorption during the water pulse and remnant water contained within the film could allow nucleation of  $\text{TiO}_2$  by reaction with  $\text{TiCl}_4$  during the subsequent  $\text{TiCl}_4$  pulse. Thus, it is necessary to adequately purge the system to ensure removal of remnant water from the film. Initial experiments were conducted with a 1-min purge time after the water pulse in order to directly compare the selectivity achieved with PMMA films relative to OTS-SAM surfaces. It was encouraging to note that PMMA films showed low nucleation after 100 deposition cycles. Figure 3 shows the comparison of Ti atom % on the PMMA surface

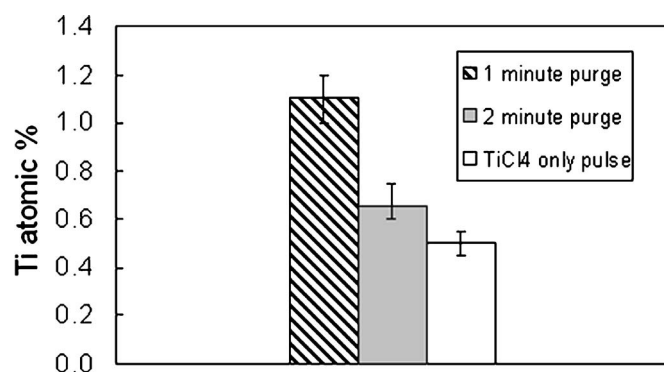


**Figure 3.** Ti atomic percent on PMMA at two different purge times after the water pulse and for the  $\text{TiCl}_4$ -only case. The pulse sequences used are (diagonal stripes) -2 s-25 s-1 s-60 s-, (gray) -2 s-25 s-1 s-120 s-, and (white) -2 s-25 s-.

at two different purge times after the water pulse. An increase in the purge time from 1 to 2 min after the water pulse reduced the Ti content on the PMMA films from 1.1 to 0.7 atom %. In addition, the Ti concentration after a 2-min water purge is very similar to the Ti atom % measured on PMMA films exposed to 150 pulses of  $\text{TiCl}_4$  only [i.e., -2 s( $\text{TiCl}_4$ )-25 s (purge)-]. Therefore, it was concluded that while using PMMA as a mask for the selective ALD process, a purge time of 1–2 min is sufficient to minimize the effect of remnant water in the PMMA film without requiring undesirably long purge and cycle times. Although there is a relative increase of almost 50% in Ti atomic surface concentration, a reduction in the purge time after the water pulse from 2 to 1 min still results in sufficient removal of remnant moisture to avoid significant spurious nucleation of  $\text{TiO}_2$  on the polymer surface. Therefore, due to the practical consideration of maintaining as short a cycle time as possible, a purge time of 1 min was used for further experiments.

In addition to reacting directly with either the polymer or remnant precursor absorbed into the polymer masking layer, it is possible that the ALD precursors can diffuse through the polymer masking layer and react directly with the substrate surface. Unlike previous efforts in which SAMs were used to passivate reactive surface functional groups by chemical reaction with the SAM, polymer films do not directly react with the substrate surface. Instead, the polymer simply physically coats the surface and serves as a diffusion barrier that physically blocks the reactive substrate surface groups from the ALD precursors. While this permits the polymer films to be easily coated and easily removed from the surface after deposition, it also means that reactive surface functional groups still exist at the bottom of the protective polymer masking layer. Therefore, in the case of the titania deposition described in this work, if the  $\text{TiCl}_4$  precursor has sufficient time to diffuse through the polymer film and reach the silicon substrate, it will react with surface hydroxyl species and nucleate growth of titania below the polymer film. Subsequently, if water also has sufficient time to diffuse through the polymer film during its pulse, titania growth will occur at the substrate surface beneath the polymer coating. Two factors are extremely important in preventing this behavior. First, the distance over which a penetrant molecule can diffuse in the polymer film during a specific time period depends on its diffusion coefficient in the polymer. Therefore, combinations of polymers and precursors which have low diffusivities for the precursor in the polymer are advantageous in reducing the impact of this particular concern. Second, the amount of time that the precursor is exposed to the substrate during each deposition cycle is also important because it controls the time scale for diffusion of the precursor to the substrate surface. Therefore, it is best to utilize precursor exposure cycle times that are as short as possible while maintaining well-controlled ALD growth. For a particular precursor–polymer combination and a specific ALD cycle time sequence, this translates into the masking layer thickness becoming the controlling parameter that determines if the polymer film can prevent the undesired growth of ALD material on the substrate beneath the polymer.

In order to investigate this issue, a series of depositions were conducted on PMMA samples of different thicknesses and possible titania growth under the polymer film was assessed. After 100 ALD cycles [2 s( $\text{TiCl}_4$ )-25 s( $\text{N}_2$ )-1 s( $\text{H}_2\text{O}$ )-60 s( $\text{N}_2$ )], the polymer film was removed using acetone and the underlying substrate surfaces analyzed by XPS. First, it was observed in the case of thicker PMMA films (180 and 420 nm) that the films were removed easily by dipping the samples in acetone and then thoroughly rinsing them with acetone, methanol, and DI water. However, in case of thinner films (32, 56, and 103 nm) it was necessary to assist the removal process by physically wiping the film off the substrate in the presence of the solvent. It has been previously reported that PMMA can strongly interact with silica surfaces and that this interaction can lead to physical property changes in ultrathin PMMA films.<sup>16,17</sup> However, the difficulty in removal of the polymer film is not simply the result of thin-film effects on the dissolution behavior of the PMMA film. Solvent removal of PMMA films at all thicknesses was



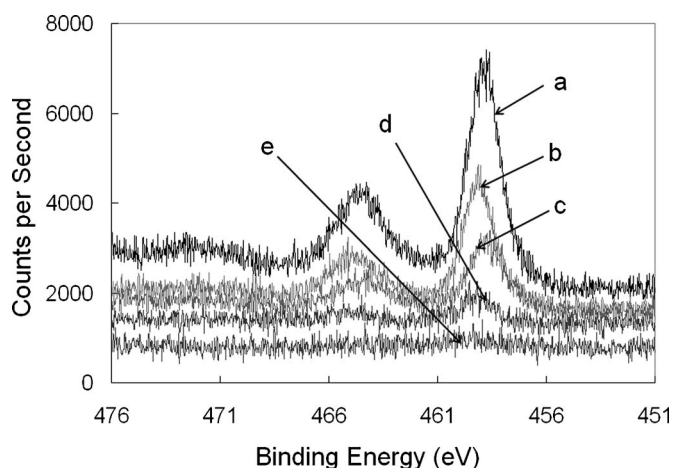


**Figure 4.** XPS spectra showing the Ti 2p peak on the substrate for different initial thicknesses of the PMMA film. The scans are taken after the PMMA film was removed from the Si wafer. Film thicknesses were: (a) 32, (b) 56, (c) 103, (d) 180, and (e) 420 nm. The spectra have been shifted vertically along the Y axis arbitrarily for purposes of separation and clearer representation.

possible using acetone when the samples were treated prior to any exposure to  $\text{TiCl}_4$ . Instead, it is believed that two phenomena are responsible for this observed difficulty in removing the thinner PMMA films: (i) titania deposition at the substrate–polymer interface and (ii) deposition of titania in the polymer near the free surface. It is believed that a lift-off mechanism is responsible for polymer removal by solvent in cases where the PMMA was exposed to a large number of ALD cycles. The polymer near the free surface also has titania incorporated into it which forms a PMMA–titania layer whose dissolution by solvent is difficult. In cases where there is a region of relatively pure PMMA under this PMMA–titania layer (i.e., the 180- and 420-nm-thick PMMA films), solvent dissolution of the pure PMMA layer can result in undercutting and lift-off of the polymer film. In cases where the PMMA film is sufficiently thin (i.e., the 32, 56, and 103-nm-thick PMMA films), it is believed that no such pure PMMA layer exists, and therefore dissolution and lift-off the polymer are inhibited. Figure 4 presents data showing that titania is clearly deposited on the silica surface in the case of the thinner PMMA films. It is even possible that the PMMA chains near the silicon surface can be covalently attached to the surface if the same  $\text{TiCl}_4$  molecule reacts with both the PMMA and the silicon surface. These observations would be consistent with the idea that no pure PMMA polymer region exists in the thinner films, which can aid in dissolution and removal of the polymer, and thus the thinner films are difficult to remove without mechanical assistance.

XPS scans were performed on the cleaned samples after polymer removal to measure the total Ti content on the surface. As mentioned previously, Fig. 4 presents the Ti 2p peak on the surface of samples after polymer removal for different initial thicknesses of the PMMA layer. As evident from the figure, noticeable amounts of Ti deposition are observed in the case of the thinner polymer samples while no Ti deposition is detectable on the 420-nm-thick samples. In addition, the amount of Ti detected on the surface scales with polymer film thickness. This is consistent with the fact that the precursor diffuses through the polymer and reacts at the interface, because higher concentrations of precursor reach the substrate surface in the case of thinner polymer films. These results demonstrate that selection of a minimum film thickness for the polymer masking layer is required for a specific polymer–precursor–cycle time process combination.

*Deposition of patterned films.*—Once the process requirements for successful selective ALD of  $\text{TiO}_2$  from  $\text{TiCl}_4$  and water vapor were established using PMMA as a masking layer, direct patterned

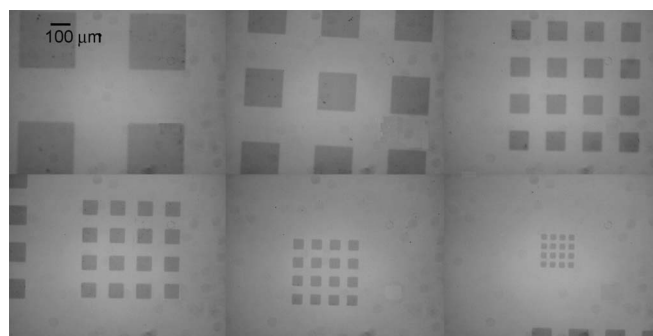


**Figure 5.** Optical micrograph of different size  $\text{TiO}_2$  patterns fabricated via area-selective ALD.

deposition of titania films was performed. PMMA films of 232 nm thickness were prepared using the procedure described earlier. The films were patterned by exposing them to approximately  $55 \text{ J/cm}^2$  of deep-UV (248-nm) light followed by development in 1:1 isopropyl alcohol/methyl isobutyl ketone (IPA: MIBK) solution for 60 s. Samples were thoroughly rinsed with IPA and DI water after removing them from the developer solution and then dried under  $\text{N}_2$ . The samples were further dried in a vacuum oven at  $100^\circ\text{C}$  for 1 h to remove residual moisture or solvent.  $\text{TiO}_2$  films were grown on the patterned substrates by depositing for 150 cycles [2 s( $\text{TiCl}_4$ )-25 s( $\text{N}_2$ )-1 s( $\text{H}_2\text{O}$ )-60 s( $\text{N}_2$ )] at  $160^\circ\text{C}$ . Following deposition, to insure complete removal of the polymer mask, the polymer was removed by first dipping the sample in warm acetone for 20 min and then sonicating in acetone for an additional 30 min. Figure 5 shows optical micrographs of various square pattern sizes obtained using this masked area-selective ALD technique. Figure 6 shows the Ti 2p XPS peak region for both the open and masked regions of the silicon substrate after  $\text{TiO}_2$  deposition and removal of the polymer mask.

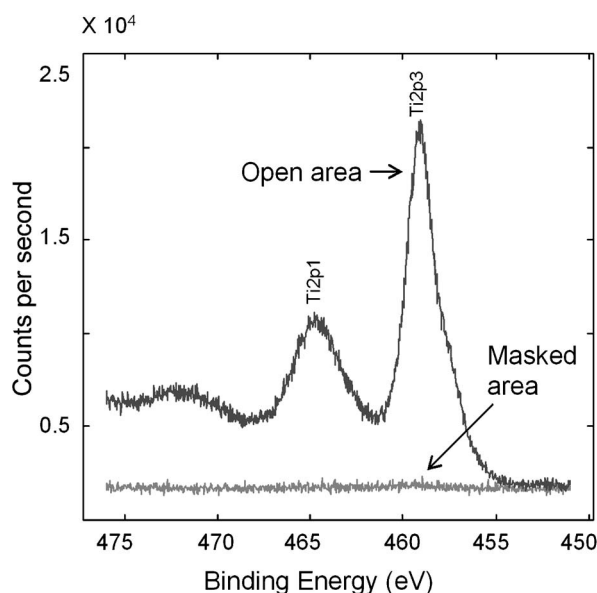


**Figure 6.** XPS scan showing the Ti 2p peak in different regions of the substrate after stripping the PMMA masking film. Open area: regions which were not covered with polymer film. Masked area: regions which were initially covered with the polymer film.

The XPS data clearly show that the patterned PMMA mask was successful in achieving area-selective ALD.

### Conclusions

A novel technique for direct patterned deposition of TiO<sub>2</sub> via area-selective ALD using PMMA as a polymer masking material has been reported. Results suggest that intrinsic reactivity of the polymer resin with the ALD precursors, presence of remnant precursors in the polymer film after each precursor pulse, and diffusion of precursor through the masking layer are critical parameters in establishing a successful polymer masked area-selective ALD process. PMMA shows low reactivity toward TiCl<sub>4</sub>, which makes it a suitable masking material for titania growth using TiCl<sub>4</sub>. PMMA also shows low water uptake and the effect of remnant water within the film can be minimized using reasonable purge times. Diffusion of precursor through the polymer film and reaction at the polymer-substrate interface can be avoided by using a sufficiently thick masking layer. These results indicate the basic feasibility of a polymer masked area-selective ALD process.

*Georgia Institute of Technology assisted in meeting the publication costs of this article.*

### References

1. M. Ritala and M. Leskela, *Handbook of Thin Film Materials*, Vol. 1, pp. 103–159, H. S. Nalwa, Editor, Academic Press, San Diego (2002).
2. M. Leskela and M. Ritala, *Angew. Chem., Int. Ed.*, **42**, 5548 (2003).
3. M. Yan, Y. Koide, J. R. Babcock, P. R. Markworth, J. A. Belot, T. J. Marks, and R. P. H. Chang, *Appl. Phys. Lett.*, **79**, 1709 (2001).
4. M. H. Park, Y. J. Jang, H. M. Sung-Suh, and M. M. Sung, *Langmuir*, **20**, 2257 (2004).
5. R. Chen, H. Kim, P. C. McIntyre, and S. F. Bent, *Appl. Phys. Lett.*, **84**, 4017 (2004).
6. M. Calistri-Yeh, E. J. Kramer, R. Sharma, W. Zhao, M. H. Rafailovich, J. Sokolov, and J. D. Brock, *Langmuir*, **12**, 2747 (1996).
7. A. Ulman, *Chem. Rev. (Washington, D.C.)*, **96**, 1533 (1996).
8. P. Silberzan, L. Leger, D. Auserre, and J. J. Benattar, *Langmuir*, **7**, 1647 (1991).
9. D. Davazoglou, I. Raptis, A. Gleizes, and M. Vasilopoulou, *J. Vac. Sci. Technol. B*, **22**, 859 (2004).
10. D. Davazoglou, S. Vidal, and A. Gleizes, *Microelectronics, Microsystems and Nanotechnology, Papers presented at MMN 2000*, Athens, Greece, Nov 20–22, 2000, pp. 131–134 (2001).
11. A. Sinha, D. W. Hess, and C. L. Henderson, *Proc. SPIE*, **5753**, 476 (2005).
12. K. Prabhakaran, Y. Kobayashi, and T. Ogino, *Surf. Sci.*, **290**, 239 (1993).
13. J. Chastain and R. C. King, Jr., *Handbook of X-Ray Photoelectron Spectroscopy*, PHI Electronics (1995).
14. R. Matero, A. Rahtu, and M. Ritala, *Chem. Mater.*, **13**, 4506 (2001).
15. J. Aarik, A. Aidla, H. Mandar, and T. Uustare, *Appl. Surf. Sci.*, **172**, 148 (2001).
16. L. Singh, P. J. Ludovice, and C. L. Henderson, *Proc. SPIE*, **5039**, 1008 (2003).
17. M. Kawaguchi, S. Yamagiwa, A. Takahashi, and T. Kato, *J. Chem. Soc., Faraday Trans.*, **86**, 1383 (1990).